NASA CONTRACTOR REPORT

NASA CR-1504

MEASUREMENTS OF THE EXTINCTION PARAMETERS OF HOT SEEDED HYDROGEN AT 1 ATMOSPHERE PRESSURE

by A. S. Shenoy, J. R. Williams, and J. D. Clement

Prepared by
GEORGIA INSTITUTE OF TECHNOLOGY
Atlanta, Ga.
for Lewis Research Center

NATIONAL AERONAUTICS AND SPACE ADMINISTRATION • WASHINGTON, D. C. • FEBRUARY 1970

1. Report No.	2. Government Accession No.	3. Recipient's Catalog No.
NASA CR-1504		

4. Title and Subtitle	5. Report Date
MEASUREMENTS OF THE EXTINCTION PARAMETERS OF HOT SEEDED HYDROGEN AT 1 ATMOSPHERE PRESSURE	February 1970
	6. Performing Organization Code
7. Author(s)	8. Performing Organization Report No.
A. S. Shenoy, J. R. Williams, and J. D. Clement	
9. Performing Organization Name and Address	10. Work Unit No.
~~The~~ Georgia Institute of Technology Atlanta, Georgia	11. Contract or Grant No. NGR-11-002-068
	13. Type of Report and Period Covered Contractor Report
12. Sponsoring Agency Name and Address National Aeronautics and Space Administration Washington, D.C. 20546	14. Sponsoring Agency Code

15. Supplementary Notes

16. Abstract

The extinction parameters of carbon-hydrogen, tungsten-hydrogen, and silicon-hydrogen aerosols were measured as a function of radiation wavelength from 1200 to 6000 Å at various temperatures up to 3450° F. The submicron-sized carbon particles have a relatively high extinction parameter of the order of 50,000 cm^2/gm. However, at higher temperatures the carbon particles disappear due to chemical reactions between hydrogen and carbon. The extinction parameter of tungsten particles was found to be about 10,000 to 20,000 cm^2/gm and that of silicon to be about 65,000 cm^2/gm. In all of these cases the extinction parameter is essentially independent of wavelength and temperature over the range of wavelengths and temperatures investigated.

17. Key Words (Suggested by Author(s))	18. Distribution Statement
Extinction parameters of particles; Radiation from hot gases with particles	Unclassified - unlimited

19. Security Classif. (of this report)	20. Security Classif. (of this page)	21. No. of Pages	22. Price*
Unclassified	Unclassified	45	$3.00

*For sale by the Clearinghouse for Federal Scientific and Technical Information
Springfield, Virginia 22151

Distribution of this report is provided in the interest of information exchange. Responsibility for the contents resides in the author or organization that prepared it.

FOREWORD

The research described herein is concerned with the extinction of thermal radiation by hot particle-seeded hydrogen and is related to advanced reactor concepts for nuclear rocket propulsion. This work was performed under NASA Grant NGR-11-002-068 with Mr. Charles C. Masser, Nuclear Systems Division, NASA Lewis Research Center as Technical Manager.

TABLE OF CONTENTS

SUMMARY

Measurements of the extinction parameter as a function of temperature and incident radiation wavelength were made of hydrogen seeded with submicron-sized particles. Hydrogen, first unseeded and then seeded, was heated in a furnace employing an electrically heated tungsten strip. Radiation of wavelengths from about 1200 Å to 6000 Å was passed through unseeded and then seeded hydrogen at a given temperature. Measurements of the transmission for the two cases yielded the extinction parameter for the particle seed in hydrogen gas.

The extinction parameters of carbon-hydrogen, tungsten-hydrogen, and silicon-hydrogen aerosols were measured as a function of radiation wavelength at various temperatures up to 3450°F. The submicron-sized carbon particles have a relatively high extinction parameter of the order of 50,000 cm^2/gm. However, at higher temperatures the carbon particles disappeared from the aerosol. Chemical analysis of the carbon-hydrogen aerosol at higher temperatures verified that methane was present, thus confirming the disappearance of carbon particles due to chemical reactions between hydrogen and carbon. In the case of tungsten particles, the extinction parameter varies from 10,000 to 20,000 cm^2/gm depending upon the size of the particles. The extinction parameter of silicon particles at room temperature is about 65,000 cm^2/gm. In all of these cases the extinction parameter is essentially independent of wavelength over the range of wavelengths and temperatures investigated.

Electron micrographs of the carbon, tungsten, and other seed materials used were taken. The electron micrographs present representations of the particles of which the extinction parameters were measured.

The measured extinction parameters of various seed materials are compared with theoretical values for spherical particles calculated using the Mie theory.

INTRODUCTION

The absorption of thermal radiation by a gas is usually greatly enhanced by the addition of very small particles of a suitable material. If the particles are small enough, they may remain essentially in thermal and dynamic equilibrium with the gas as the gas is heated by radiation to the particles with subsequent conduction from the particles to the gas.[1,2] Particle-seeded hydrogen is currently being considered as the propellant for the gaseous core nuclear rocket.

Two gaseous core nuclear reactor concepts that are currently being investigated for nuclear rocket propulsion are the coaxial flow reactor,[3-6] in which a slow moving central stream of gaseous fissioning fuel heats a fast moving annular stream of particle-seeded gas primarily by thermal radiation, and the nuclear light bulb reactor,[7,8] in which fissioning fuel is contained in a transparent partition and a particle-seeded gas is heated by thermal radiation through the partition. The particles in the gas are necessary to insure sufficient radiant heat transfer to the working fluid and to minimize heating of the containment vessel.[9] The performance of a gaseous core nuclear rocket would be far superior to any present-day rocket,[10,11] chemical or nuclear.

Since a gas-core nuclear rocket would rely on thermal radiation from the hot fissioning core to heat the hydrogen propellant, particle seeding is essential to its operation. Whereas gases alone tend to absorb thermal radiation in lines and bands, the absorption characteristics of particle clouds vary only gradually with wavelength.[12-14] Particle clouds of some refractory materials have been shown to have very high absorption coefficients such that only a very small mass fraction of such a particle seed material dispersed in a gas will make the gas highly absorbing.[15-16]

Radiant energy absorption by particle clouds has been investigated for many years by many people. A rigorous solution of Maxwell's equations for the absorption and scattering of radiant energy by spherical particles was published in 1908 by Mie,[17] and since that time a considerable amount of effort has been spent solving the Mie equations under various conditions.[18,19] Since the gaseous core nuclear rocket would utilize particle-seeded hydrogen

as the propellant, work was recently begun at Georgia Tech to measure the absorptive properties of hydrogen seeded with submicron-sized particles at high temperatures and pressures. In order to better understand the experimental data and to make a judicious choice of seed materials, the Mie equations were solved for some of the seed materials used in these experiments.[20]

The extinction parameters of submicron-sized particles of carbon, silicon, and tungsten suspended in hydrogen have been measured over a range of temperatures to 3450°F. The submicron-sized carbon particles were found to have a relatively high extinction parameter of about 50,000 cm^2/gm. However, at temperatures above 1000°F the carbon particles tended to react with the hydrogen to produce methane. In the case of tungsten particles, the extinction parameter varied from 10,000 cm^2/gm to 20,000 cm^2/gm depending upon the nominal size of the particles. The extinction parameter of silicon particles was found to be about 65,000 cm^2/gm. In all of these cases the extinction parameter is essentially independent of wavelength over the range of wavelengths and temperatures investigated.

GENERAL BACKGROUND

There are three significant mechanisms by which radiant energy interacts with a gas containing particles: (1) absorption by the gas, (2) absorption by the particles suspended in the gas, and (3) scattering by the particles. The importance of each of these three mechanisms depends on the composition, temperature and pressure of the gas, the composition, sizes and shapes of the particles, the particle number density, and the spectrum of the radiant energy.

The attenuation of a beam of monochromatic radiant energy by a gas containing particles is governed by the expression

$$I(\lambda,x) = I(\lambda,o)\, e^{-k_T(\lambda)x} \tag{1}$$

where $k_T(\lambda)$ is the total linear attenuation coefficient for radiant energy of wavelength λ, and x is the distance the beam traverses through the seeded gas. The total linear attenuation coefficient for all three interaction processes is equal to the sum of the linear attenuation coefficients for each process separately, that is,

$$k_T(\lambda) = k_a^g(\lambda) + k_a^p(\lambda) + k_s^p(\lambda) \tag{2}$$

where $k_a^g(\lambda)$ is the linear attenuation coefficient due to absorption by the gas alone, $k_a^p(\lambda)$ is the linear attenuation coefficient due to absorption by the particles, and $k_s^p(\lambda)$ is the linear attenuation coefficient due to scattering by the particles. $k_a^p(\lambda)$ and $k_s^p(\lambda)$ are proportional to the number density of the particles as long as the particles are randomly oriented and the average distance between the particles is much greater than their effective radius, so it is convenient to define the absorption parameter $\mu_a(\lambda)$ and scattering parameter $\mu_s(\lambda)$ by

$$\mu_a(\lambda) = \frac{k_a^p(\lambda)}{\rho} \text{ and } \mu_s(\lambda) = \frac{k_s^p(\lambda)}{\rho} \tag{3}$$

where ρ is the particle density in grams of particles per cubic centimeter of aerosol. $\mu_a(\lambda)$ is also called the mass absorption coefficient. The totality of processes by which energy is removed from a beam by a particle cloud is called extinction, so the extinction parameter is given by

$$\mu_e(\lambda) = \mu_a(\lambda) + \mu_s(\lambda) \ . \qquad (4)$$

The absorption, scattering, and extinction parameters are independent of the concentration of particles.

One may now consider the absorption of radiant energy by particle-seeded gases to be the sum of two independent processes; absorption by the gas itself and absorption due to the particles in the gas. The absorption coefficient of the gas, $k_a^g(\lambda)$, depends only on the composition, temperature, and pressure of the gas; whereas the absorption and scattering parameters of the particles, $\mu_a(\lambda)$ and $\mu_s(\lambda)$, depend on the composition, sizes, and shapes of the particles. Thus, $k_a^g(\lambda)$ may usually be determined for the pure gas and $\mu_a(\lambda)$ and $\mu_s(\lambda)$ for the particles in any transparent medium and then $k_T(\lambda)$ is calculated for the particle-seeded gas using equations 2 and 3. However, this procedure becomes difficult, if not impossible, when the composition of the gas and the sizes and shapes of the particles are changed by chemical reactions between the particles and the gas.

The basic mechanisms of radiant energy absorption by particle clouds and by gases are quite different. Since atoms and molecules of a gas absorb radiant energy in discrete quanta, the absorption coefficient of a gas may change many orders of magnitude over a wavelength interval of a few Angstroms. The familiar absorption spectra of various gases attest to the wide variations of $k_a^g(\lambda)$ as λ is changed.

Whereas gases tend to absorb in lines and bands, the absorption and scattering characteristics of particle clouds vary only gradually with the wavelength of the incident radiant energy. Thus, $\mu_a(\lambda)$ and $\mu_s(\lambda)$ are smoothly varying functions of wavelength. Scattering enhances energy absorption in particle clouds by increasing the average path length traversed by the radiant energy. However, in any given unit volume of aerosol, the particle-gas mixture is heated only by absorption, not by scattering. For this reason it is convenient to define the absorption coefficient for the

aerosol, $k_a(\lambda)$, by

$$k_a(\lambda) = k_a^g(\lambda) + k_a^p(\lambda) = k_a^g(\lambda) + \rho\mu_a(\lambda) \ . \tag{5}$$

Then the scattering coefficient for the aerosol is equal to the scattering coefficient of the particles alone, since scattering by the gas is negligible.

$$k_s(\lambda) = k_s^p(\lambda) = \rho\mu_s(\lambda). \tag{6}$$

The effect of scattering depends not only on the value of $\mu_s(\lambda)$ but also on the angular dependence of the scattered energy. Scattering from small particles is usually highly anisotropic.

A rigorous solution to Maxwell's equations for the absorption and scattering of radiant energy by homogeneous spherical particles of any composition suspended in a homogeneous nonmagnetic transparent medium was published in 1908 by Gustav Mie[17] and is now commonly known as the Mie theory. Krascella[14] applied a transformation procedure developed by Aden[19] to the Mie equations to calculate the effect of particle size, wavelength, and particle temperature on particle opacity in those regions of the ultraviolet, visible, and infrared spectra for which complex index of refraction data were available. The authors have used Krascella's program to extend these calculations to other types of particles and to a broader wavelength range.[20]

Svatos[21] has recently published a solution to Maxwell's equations for extinction by flattened ellipsoids; however, at present there is no theory to accurately predict the absorption and scattering characteristics of irregularly shaped particles. The Mie theory predicts that $\mu_a(\lambda)$ is a maximum when the particle radius is of the order of the wavelength λ divided by 2π. Thus, for a given particle seed density ρ, the absorption of thermal radiation in the near infrared, visible, and ultraviolet regions of the spectrum is greatest for submicron-sized particles of diameters in the range of 0.05 to 0.25 micron. Submicron-sized particles of refractory materials are generally highly irregular in shape, so the Mie theory can only be used as an approximation to the absorption and scattering characteristics of these particles.

INSTRUMENTATION AND EQUIPMENT

Hydrogen, first unseeded and then seeded, is heated in the furnace to temperatures up to about 5000°R by an electrically heated tungsten strip. A beam of radiant energy from a capillary discharge tube passes first through unseeded and then seeded hydrogen at a given temperature (Figure 1). Radiant energy passing through the furnace falls on the diffraction grating and is focused on photomultiplier 1 in Figure 1. Measurements of the transmission for the two cases yield the extinction parameter of the hot seeded hydrogen. A small portion of the beam is diverted by a pair of mirrors (not shown in Figure 1) to photomultiplier 2 to monitor changes in the aerosol concentration. There is another aerosol monitor at the entrance of the furnace (Figure 2) to monitor the cold aerosol. A two watt concentrated zirconium arc lamp is employed as a light source. This light passes through the cold aerosol and is monitored by a third photomultiplier tube. Outputs from these three photomultiplier tubes are amplified by picoammeters and recorded by an oscillograph.

The drive mechanism shown in Figure 1 consists of a 75 rpm synchronous reversible motor which drives a shaft to turn the diffraction grating to scan the spectrum to 6000 Å. Limit switches on the drive mechanism limit the traverse of the drive shaft and automatically reverse the rotation of the grating after the spectrum has been scanned in the forward direction in order to scan the spectrum in the reverse direction. At the end of the reverse scan, the limit switch shuts off the motor. Initially, a push button switch starts the drive of the visicorder and the synchronous motor.

The mixture of submicron-sized particles and hydrogen is produced by an aerosol generator. The aerosol generator essentially consists of a chamber in which submicron-sized particles are mixed with hydrogen by blades driven by a motor. This mixture at a pressure of about 400 psi or more is passed through a nozzle before entering the furnace to further deagglomerate the particles.

The experimental setup is located in a laboratory of 12 feet by 24 feet. Since hydrogen is an explosive gas, the room is partitioned by a double

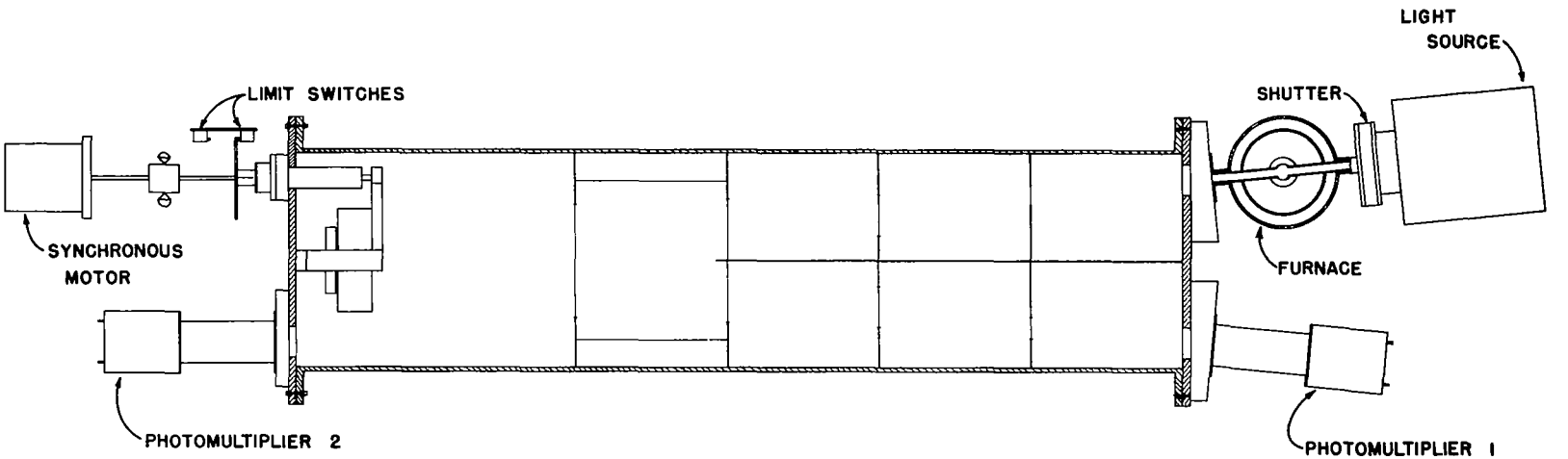

Figure 1. Monochromator Assembly

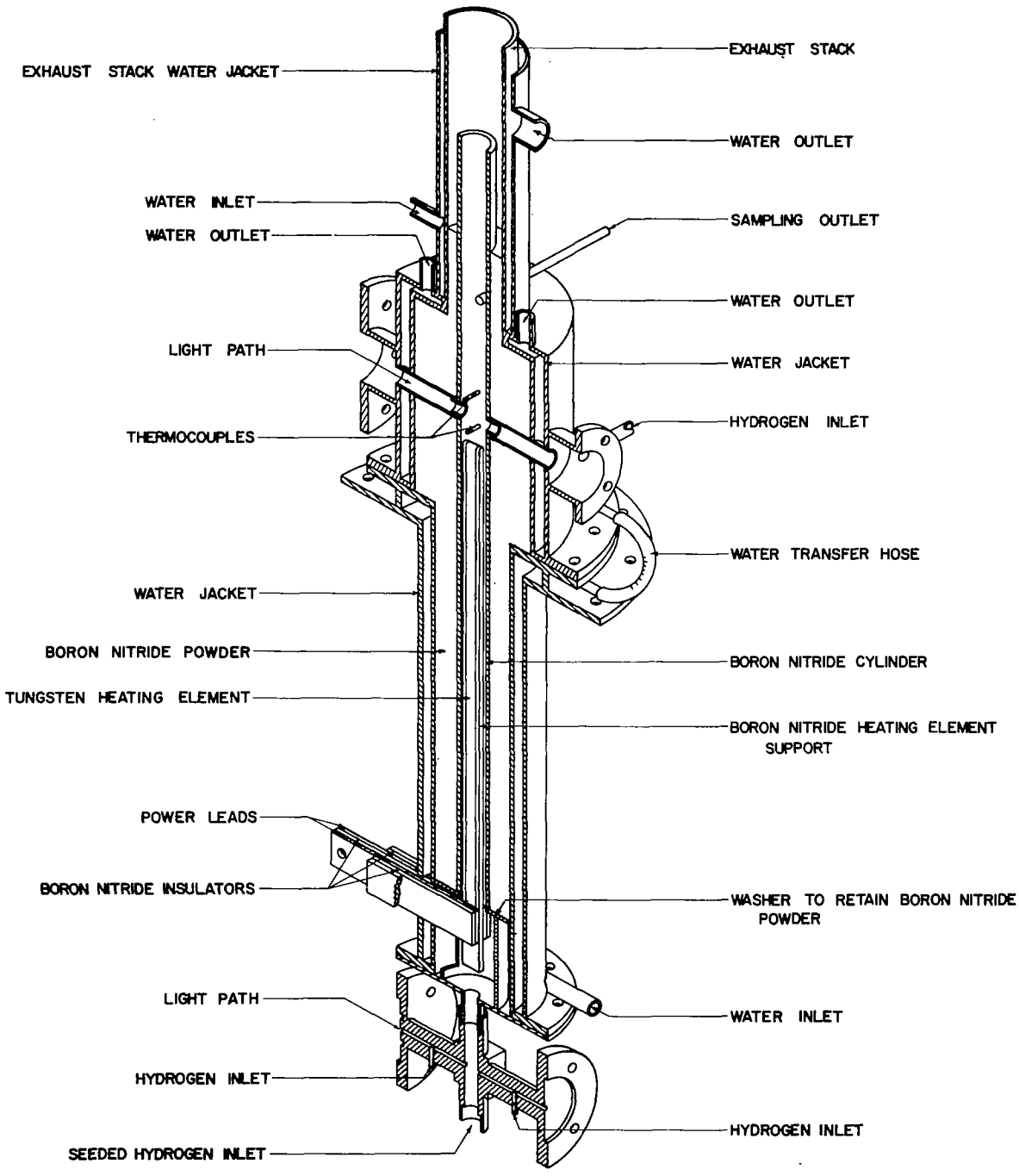

Figure 2. Furnace Assembly

thickness aluminum wall which forms a hood and separates personnel from the equipment. On one side of the wall the control console, data recording table, and gas control system are located, and on the other side of the wall the experimental equipment is located. This enables the operator to conduct the experiment remotely from the control console safely. The wall contains a double thickness Plexiglas window to allow observation of the equipment while data are being taken. In order to avoid a buildup of hydrogen, this hood utilizes a large capacity fan which exhausts to the outside.

The high temperature furnace is designed to heat the aerosol mixture to temperatures of the order of 5000°R. Figure 2 illustrates the furnace. There are two positions where the transmission of light is measured; at the bottom where the aerosol enters, and at the top after the aerosol has been heated.

The heating element is a two and one-half foot long by five-eighths inch wide strip of 25 mil thick tungsten. The ends of the heating element are connected by copper power leads to a 20 kilowatt dc power supply. Supporting the tungsten heating element is a one-eighth inch thick hot pressed boron nitride strip. The whole heating element is contained in a five-eighths inch ID boron nitride tube in which the aerosol is heated. By varying the flow rate of aerosol and the heater voltage, the desired temperature is attained.

The one inch OD boron nitride tube is placed in a water jacket. The annular space between the boron nitride tube and water jacket is filled with boron nitride powder to serve as insulation. The copper water jacket is made in two parts so that the furnace can be disassembled and reassembled easily. The furnace is designed so that the filament can be easily replaced when it burns out.

After it passes between the observation tubes, the aerosol exhausts to an aerosol disposal system. There are two sampling systems used to simultaneously measure the concentration of seed material in the hydrogen. One sample is taken at the entrance of the furnace and the other sample is taken near the exhaust. These two samples are used to study the effect of temperature on seed vaporization.

Temperature measurements are made with tungsten three percent rhenium

versus tungsten 26 percent rhenium thermocouples. These thermocouples are capable of operation in hydrogen at 5000°F. The temperatures are measured immediately below the light beam and immediately above the light beam with two thermocouples.

The light source which is used in the ultraviolet and visible regions of the spectrum is a gas discharge lamp. Figure 3 shows the sectional view of the light source and its connection to the furnace. The light source has a three-sixteenths inch diameter glass capillary discharge tube which is cooled by water and has an aluminum cathode which is air cooled by a fan in the lamp housing. The light source is capable of handling 1000 watts of energy continuously.

The monochromator is illustrated in Figure 1. The main chamber is constructed from a stainless steel tube 10.75 inches in outside diameter with a wall thickness of 0.165 inch. One-quarter inch thick flanges are welded to the tube ends, giving an overall length of 42 inches. One-half inch thick stainless steel plates for mounting the grating holder at one end of the tube and the entrance and exit slits at the other are sealed by O-rings to the flanges by means of 16 three-eighths inch bolts. Four baffles are equally spaced inside the chamber to minimize the unwanted light arriving at the exit slits.

The aluminum grating holder shown in Figure 1 is bolted directly to the end plates. The grating is a Bausch and Lomb replica grating with a one meter radius of curvature and a groove spacing of 600 lines per millimeter. The grating is rotated by advancing a finely-threaded drive rod through the end plate. The rod is spring-loaded against an arm on the grating mount. The drive rod is turned by a synchronous motor by means of a pin and slot drive. There are two limit switches which operate relays to reverse and stop the dc motor. On pressing a contact switch at the operating console, the drive motor starts scanning the spectrum, and when it reaches the end of the spectrum, the limit switch reverses the direction of the motor thereby bringing the grating to the original position. As the drive shaft comes to the initial position, the other limit switch reverses and stops it so that it is ready for another spectrum scan.

A mechanical vacuum pump is connected to the monochromator which maintains a pressure of about one micron of mercury in the chamber. The chamber

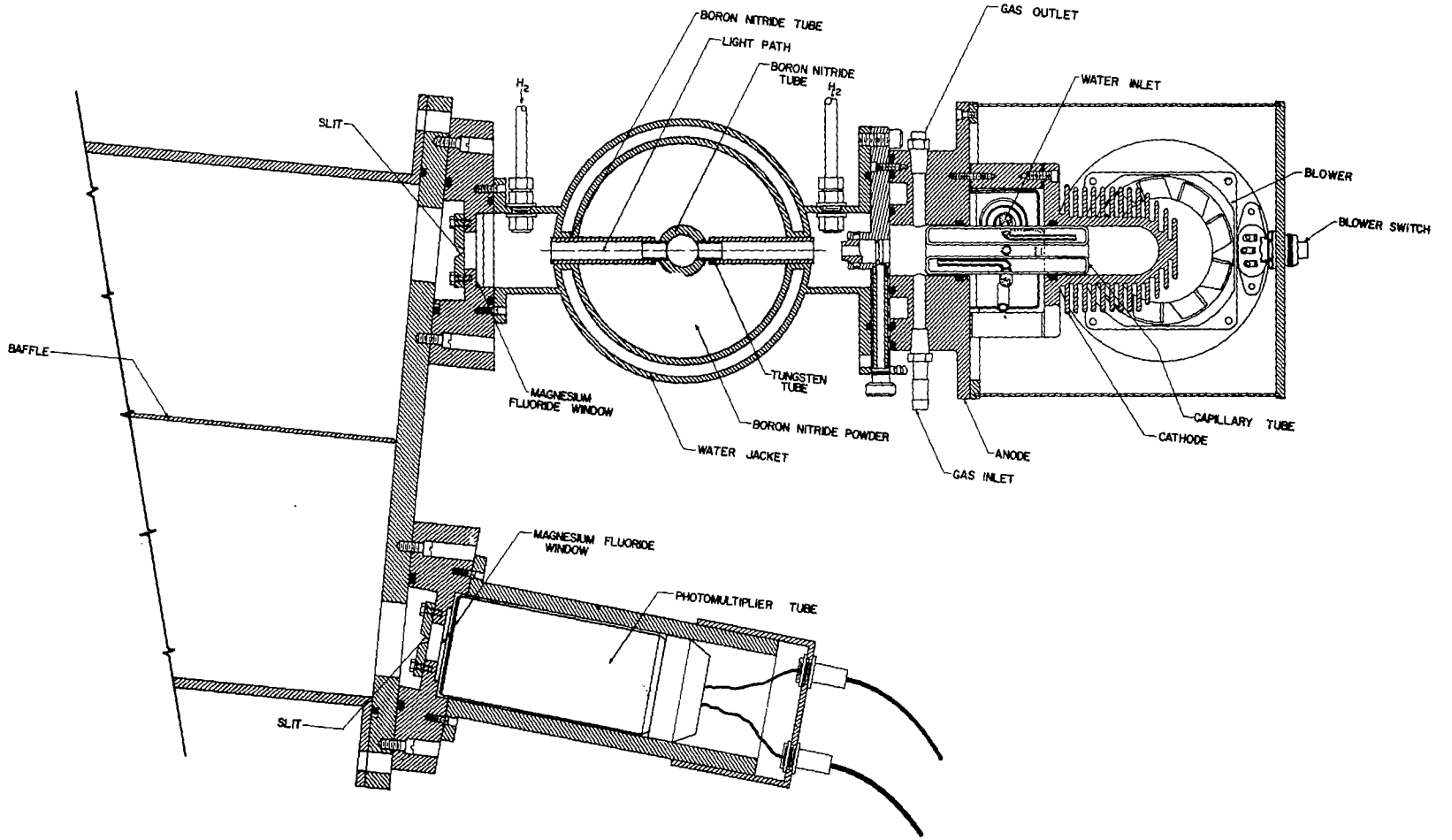

Figure 3. Spectrometer Assembly - Furnace End

pressure is measured by means of a thermocouple vacuum gauge and indicated by a meter at the operating console.

The furnace is connected to the spectrometer at an angle of six degrees to the axis as shown in Figure 3. The ray of light passing through the furnace falls on the grating and is diffracted to the photomultiplier. A small portion of the beam is diverted by a pair of mirrors to pass through a far ultraviolet bandpass filter to another photomultiplier tube to monitor the changes in the aerosol concentration.

The aerosol generator design is shown in Figure 4. The gas is introduced above the motor and flows past a loose Teflon seal on the rotating shaft into the mixing chamber. The mixing chamber is initially filled approximately one-third full with seed material, and the mixing blades which rotate at 1200 rpm mix the seed particles with the gas. The aerosol exits the mixing chamber through the outlet tube near the center of the chamber. The larger particles and agglomerates are thus discriminated against through the centrifugal action of the mixing blades. The highest degree of dispersion is obtained by allowing the aerosol to expand through a small orifice. The aerosol generator is operated at a pressure of 300 to 1000 psi. The nozzles used have orifices of 0.00635 inch and 0.0135 inch in diameter, the smaller nozzle orifice being used at higher pressures.

The aerosol concentration, in grams of seed material per cubic centimeter of aerosol, is measured by passing a known volume of aerosol through a filter and measuring the weight of seed material deposited on the filter. The concentration is then the weight of deposited seed material divided by the volume of gas passing through.

It is desirable to have some idea of the sizes and shapes of the particles produced by the aerosol generator and also to observe the degree of deagglomeration accomplished by the nozzle in the aerosol stream. The simplest method of sampling is simply by introducing an electron microscope grid in a moving aerosol and allowing particles to collect upon the grid. It was felt, however, that aerodynamic effects would favor the deposition of the larger particles while the smaller particles remained in the aerosol. Similar problems existed for a gravity-based "settling out" method which would also be inaccurate due to particle reagglomeration.

A method which overcomes these problems is electrostatic sampling. A 75 kV

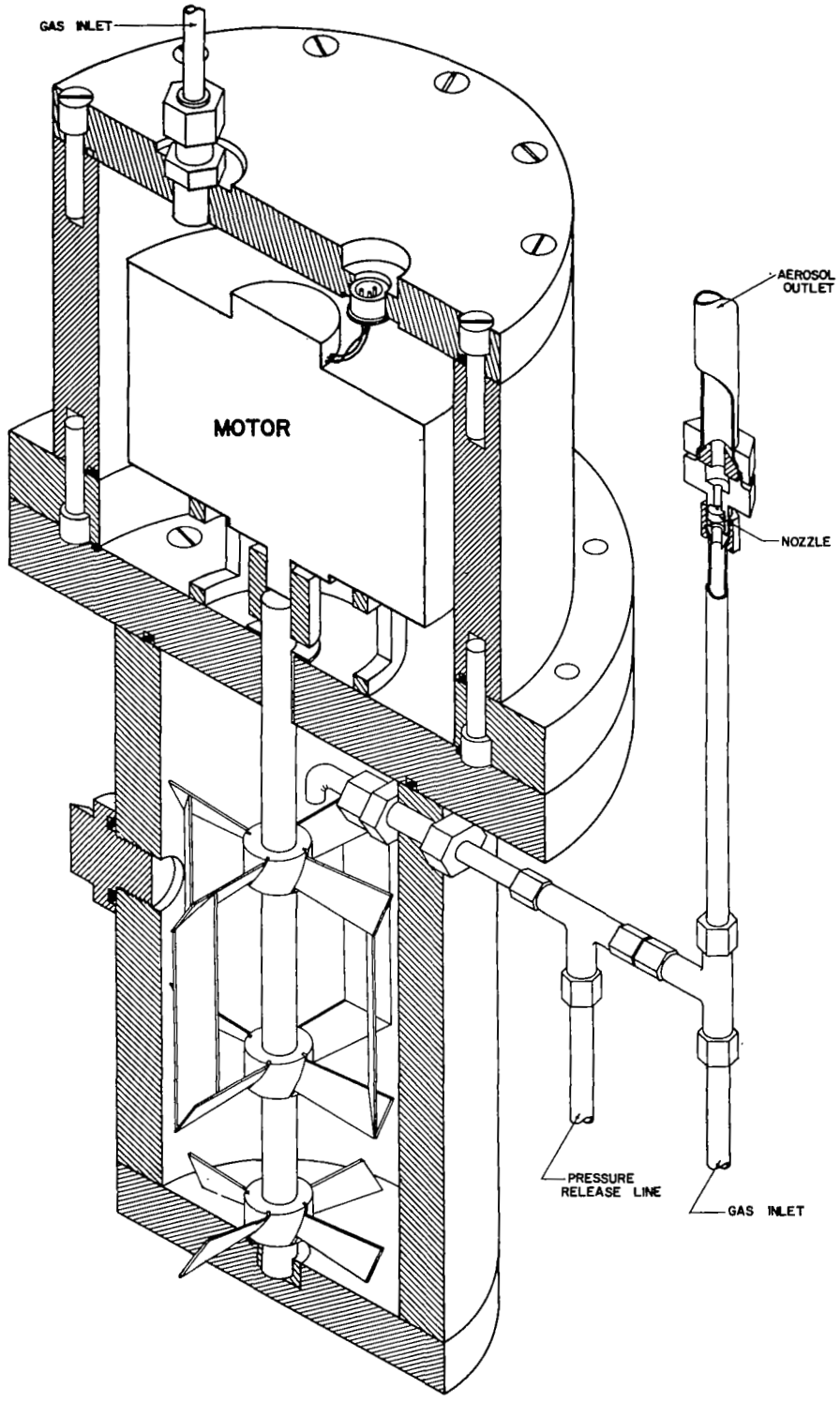

Figure 4. Aerosol Generator

Van de Graaff generator was used to provide the required voltage drop. A Plexiglas container was built with inlet and outlet ports for the gas, a needle for distribution of the negative charge obtained from the Van de Graaff generator, and a grounded metal plate upon which the metal electron microscope grids were placed. The grids are taped to the vertical base of the container so that gravity-induced precipitation does not affect the results. The grids are also located parallel to the flow, so that aerodynamic precipitation can be considered minimal.

The detector system consists primarily of three photomultiplier tubes. The first photomultiplier tube produces a signal proportional to the intensity of the diffracted light of a particular wavelength which has passed through the hot aerosol. The second photomultiplier produces a signal proportional to the intensity of a fixed narrow wavelength range in the far ultraviolet transmitted through the aerosol to monitor the aerosol concentration. The third photomultiplier gives a signal proportional to the intensity transmitted through the aerosol just before entering the furnace.

The photomultiplier tube outputs are monitored by Keithley picoammeters. The first photomultiplier output which is wavelength dependent varies by several orders of magnitude during the scanning of the spectrum, so its output is monitored by a Keithley automatic ranging picoammeter which automatically measures currents from 10^{-13} ampere full scale to 10^{-2} ampere rapidly and accurately. The outputs of all three picoammeters are recorded by an oscillograph.

A control system capable of operating the equipment from a remote location is required for safety considerations. The operating station is located in front of an aluminum wall constructed to shield personnel from the equipment containing hot hydrogen. The design philosophy is to provide remote operation for all equipment functions that need to be varied during data collection or while either hydrogen gas is flowing or the heater element is energized.

The control system is interlocked with a safety "SCRAM" system that controls electrical power to the equipment. In the event of a power failure or a "SCRAM" signal, all electrical power to the equipment is interrupted and locked off until manually reset. Interrupting the electrical power deactivates a system of normally closed solenoid valves on all hydrogen gas lines

and also the high pressure gas lines. The water coolant to the furnace and the exhaust fan remain on.

The exhaust from the furnace is connected to a disposal system outside the building by a one and one-half inch diameter stainless steel flexible hose and copper tube. The hot seeded hydrogen, after passing through the furnace, is bubbled through water in a disposal tank. The particles remain in the water as the hydrogen bubbles rise to the surface. A blower directs air onto the surface to dilute the hydrogen by a factor of several hundred and expels it to the atmosphere. The water trap also prevents air from diffusing back into the furnace and creates a back pressure. The creation of this slight positive pressure prevents air from getting into the system should a leak occur.

DATA REDUCTION AND ANALYSIS

The signals from the three photomultiplier tubes recorded by the oscillograph are analyzed to calculate the linear attenuation coefficient of the aerosol at a given temperature for various radiation wavelengths. The extinction parameter is calculated by dividing the linear attenuation coefficient by the aerosol density. Figure 5 shows a plot of the signals from the three photomultipliers in three sections. The first section presents data collected with pure hydrogen without any particles, the second section presents data collected with particles in the gas, and the third section presents data collected a second time without particles. This last set of data is taken to make sure that no seed material has been deposited in the light path. In each section, the spectrum is scanned twice; first, in the forward direction and then in the reverse direction. During the forward scan, the shutter between the light source and the furnace is open so that photomultipliers 1 and 2 measure both the light and the thermal background radiation from the furnace. During the reverse scan, the shutter between the light source and the furnace is closed so that photomultipliers 1 and 2 measure only the thermal background from the furnace. The thermal background is more significant at higher temperatures, especially when particles are in the hydrogen.

When data are taken with particles in the hydrogen, samples are collected during the forward scan. Each scan requires exactly the same length of time, about 25 seconds. Since the synchronous motor which turns the grating runs at a constant speed, a linear plot of intensity versus wavelength is obtained from the photomultiplier 1 signal recorded by the oscillograph.

In order to calculate the extinction parameter at various wavelengths, the intensities from the three photomultiplier tubes are read from each of the six plots of intensity versus wavelength. The linear attenuation coefficient, $k(\lambda)$, is then calculated at various wavelengths taking into account the variations of the aerosol concentration and the thermal background. The density, ρ_H, of the hot aerosol is evaluated at each wavelength using the recorded data and the average mass density measured by the aerosol sampling system. The extinction parameter is then calculated from

$$\mu_e(\lambda) = \frac{k(\lambda)}{\rho_H(\lambda)} \cdot \tag{7}$$

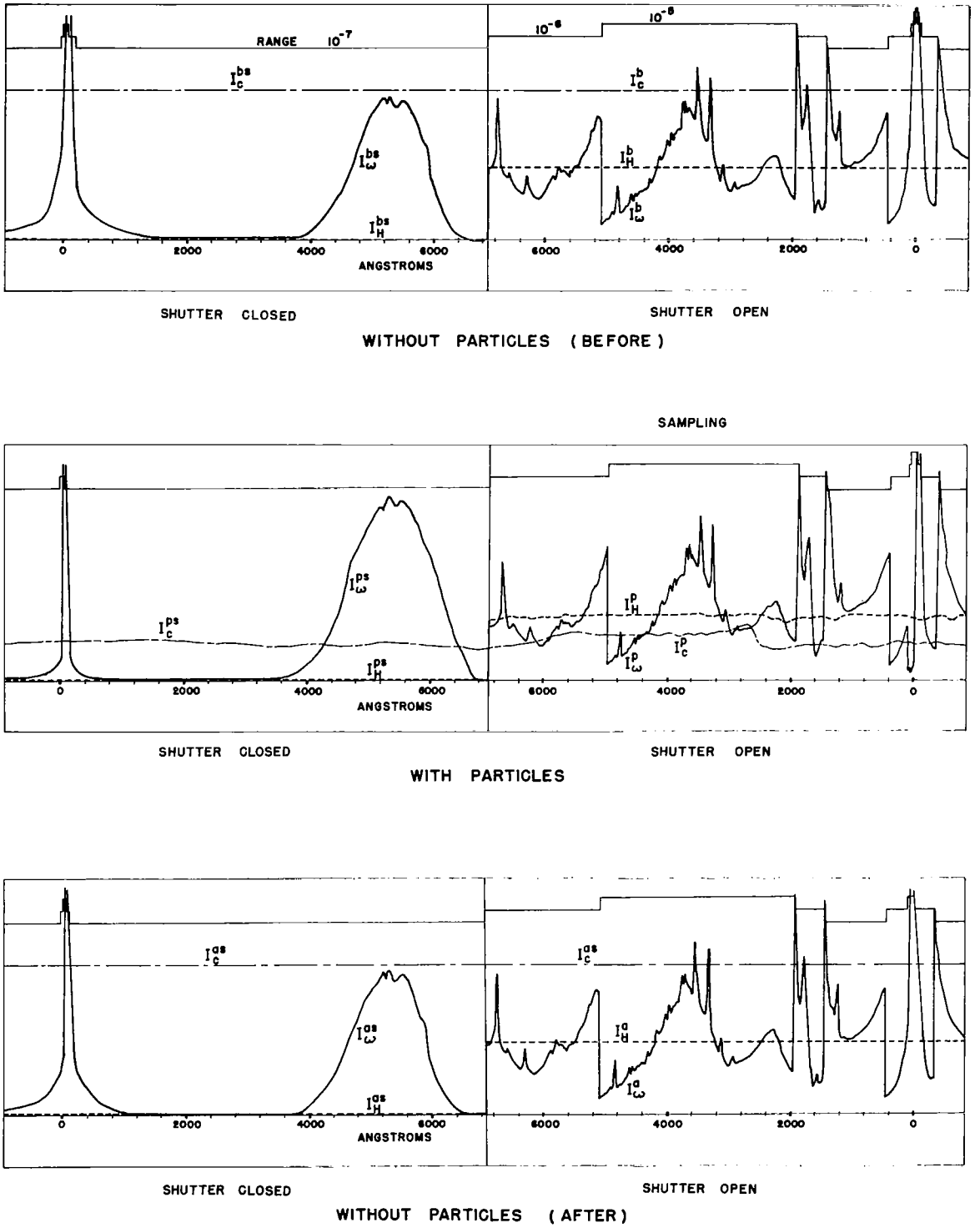

Figure 5. Oscillograph Output

The error in the extinction parameter is calculated using the errors for each piece of data used in the analysis. These calculations are carried out using the Univac 1108 at Georgia Tech. The data analysis procedure and computer program are described in detail in reference 16.

EXPERIMENTAL RESULTS

The principal properties to be considered in selecting a seed material are high absorption parameter, high melting and boiling point temperature, low neutron absorption cross section, and low reactivity with hydrogen. To obtain a higher absorption parameter, seed materials of submicron-sized particles are used. For the various submicron-sized powders, even of the same material produced by different processes, properties such as particle size, shape, color, density, and composition vary from one type of powder to another. Since the absorption parameter of any particle seed depends on these factors, it is important to specify the properties of a particular seed material used. Various types of submicron-sized carbon powder are manufactured by converting hydrocarbons to elemental carbon and hydrogen. But the properties of these powders depend on the type of process used in converting hydrocarbons to carbon. The properties of various seed materials used in seeding the hydrogen in the experiment are given in Appendix A.

In general, aerosols of submicron-sized particles can be produced by a number of methods. Since smaller particles tend to have a higher absorption parameter, the aerosol produced should contain well dispersed particles. The mixture of hydrogen and particles from the aerosol generator is expanded through a nozzle as shown in Figure 4 to allow the shear forces to further deagglomerate the particles. The degree of deagglomeration of the particles has been studied by making electron micrographs. Some electron micrographs of various seed materials are shown in Appendix B. From these electron micrographs it can be seen that the individual carbon particles are fairly spherical. The particles that are produced by blowing gas over the powder in a test tube are generally fairly large agglomerates. Electron micrographs indicate that aerosols produced by the aerosol generator and passed through the nozzle consist of highly dispersed particles. In the case of tungsten particles, the shape of individual particles is much more irregular than for carbon. It is rather difficult to define the size of such irregularly shaped particles. The electron micrographs illustrate the size and size distribution of the particles used in the experiment.

The extinction parameter of carbon aerosols has been measured for carbon of two varieties at temperatures up to 3450°F. The extinction parameter was

also measured for tungsten-hydrogen aerosols at temperatures to 3000°F and a silicon-hydrogen aerosol at room temperature.

Carbon was first used as a seed material due to its high absorption parameter, high sublimation temperature, and low neutron absorption cross section. The extinction parameter was measured for Cabot Corporation Spheron 6 and Carbolac 2 carbon black. The extinction parameter of carbon (Spheron 6) is presented as a function of radiation wavelength in Figure 6 at temperatures of 1130°F, 1480°F, and 1560°F. The extinction parameter of spherical carbon particles of 0.025 and 0.10 micron diameter was calculated using the Mie theory and is also plotted in Figure 6. The extinction parameter of carbon (Carbolac 2) is presented in Figure 7 as a function of radiation wavelength at temperatures of 2560°F, 2620°F, and 3450°F. The results indicate the extinction parameter of the carbon-hydrogen aerosol to be essentially independent of wavelength over the range of wavelengths and temperatures investigated. The results also indicate that Carbolac 2 has a slightly higher extinction parameter compared with Spheron 6. This is essentially because of the smaller particle size of Carbolac 2 compared to Spheron 6.

It was found that the density of the aerosol entering the furnace had to be increased tremendously in order to make attenuation measurements at higher temperatures. The decrease in the aerosol density was much greater than that which would have been expected due to thermal expansion of the gas alone. It is thought that the additional seed material entering the furnace at higher temperatures serves to produce sufficient concentrations of the reaction products to slow down the reaction rate so that the remaining unreacted particles are observed when the attenuation is measured. The decrease in aerosol concentration is measured by taking simultaneous samples before and after the aerosol is heated.

To confirm the disappearance of carbon particles in hydrogen, the linear attenuation coefficient for a given aerosol concentration was measured at different temperatures. At all temperatures the aerosol concentration entering the furnace was maintained constant. Figure 8 shows the linear attenuation coefficient plotted for a hydrogen-carbon aerosol and a nitrogen-carbon aerosol. The experimental values are corrected for the change in the concentration of aerosol due to the thermal expansion of the gas. In the case of the hydrogen-carbon aerosol, the linear attenuation coefficient decreases drasti-

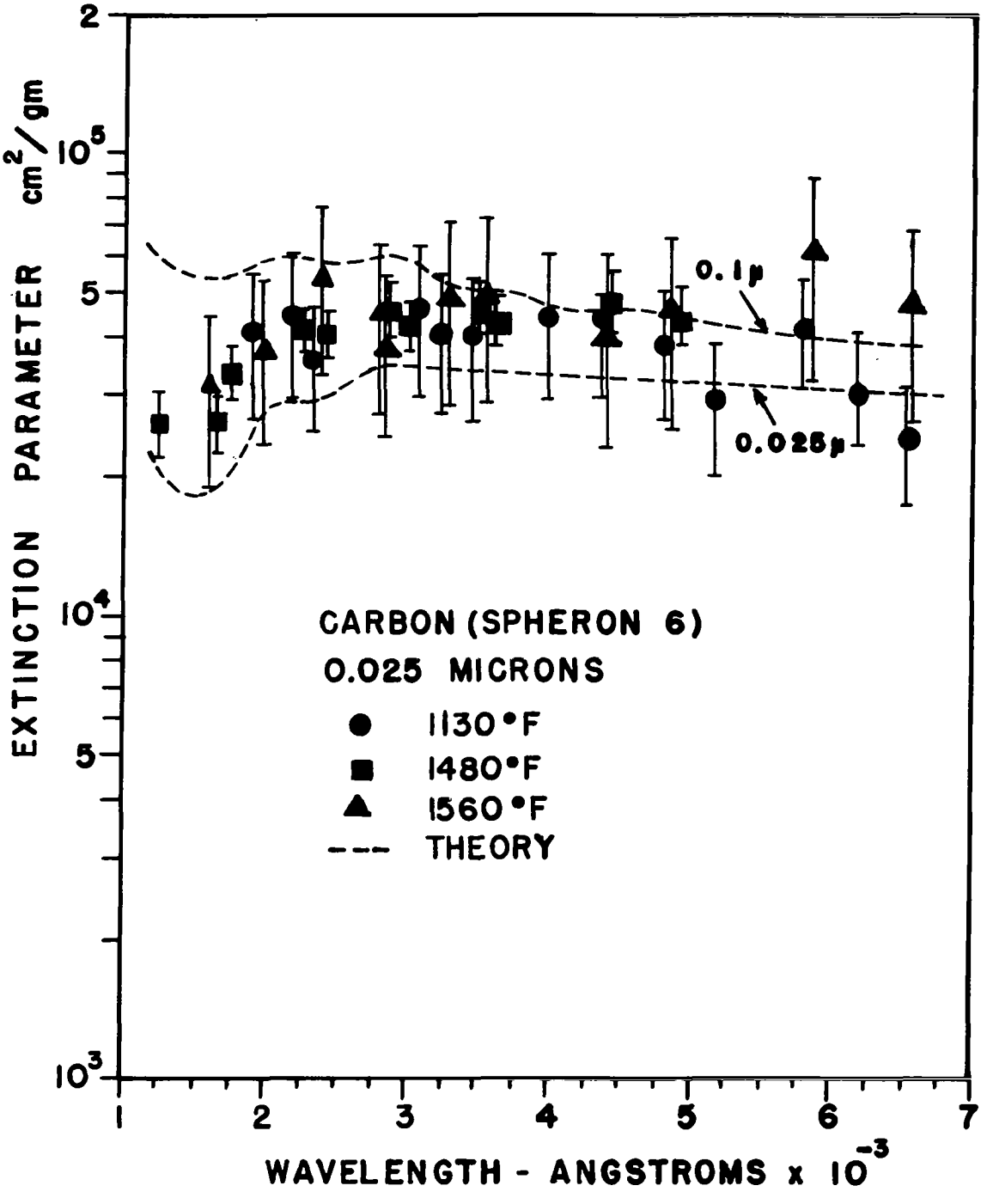

Figure 6. Comparison of the Theoretical Extinction (Absorption + Scattering) Parameter of Carbon Particles with Experimental Values

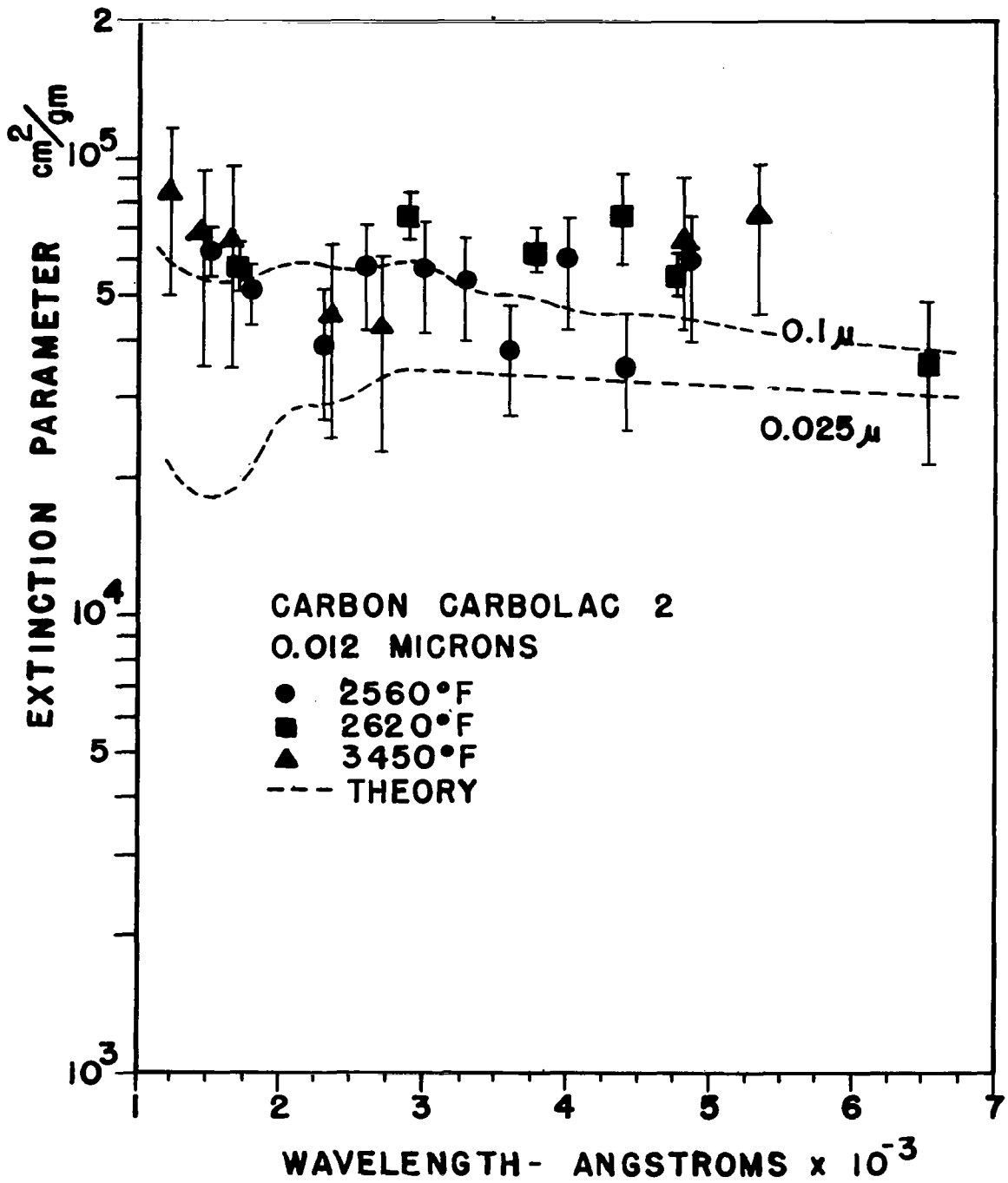

Figure 7. Comparison of the Theoretical Extinction Parameter of Carbon Particles with Experimental Values

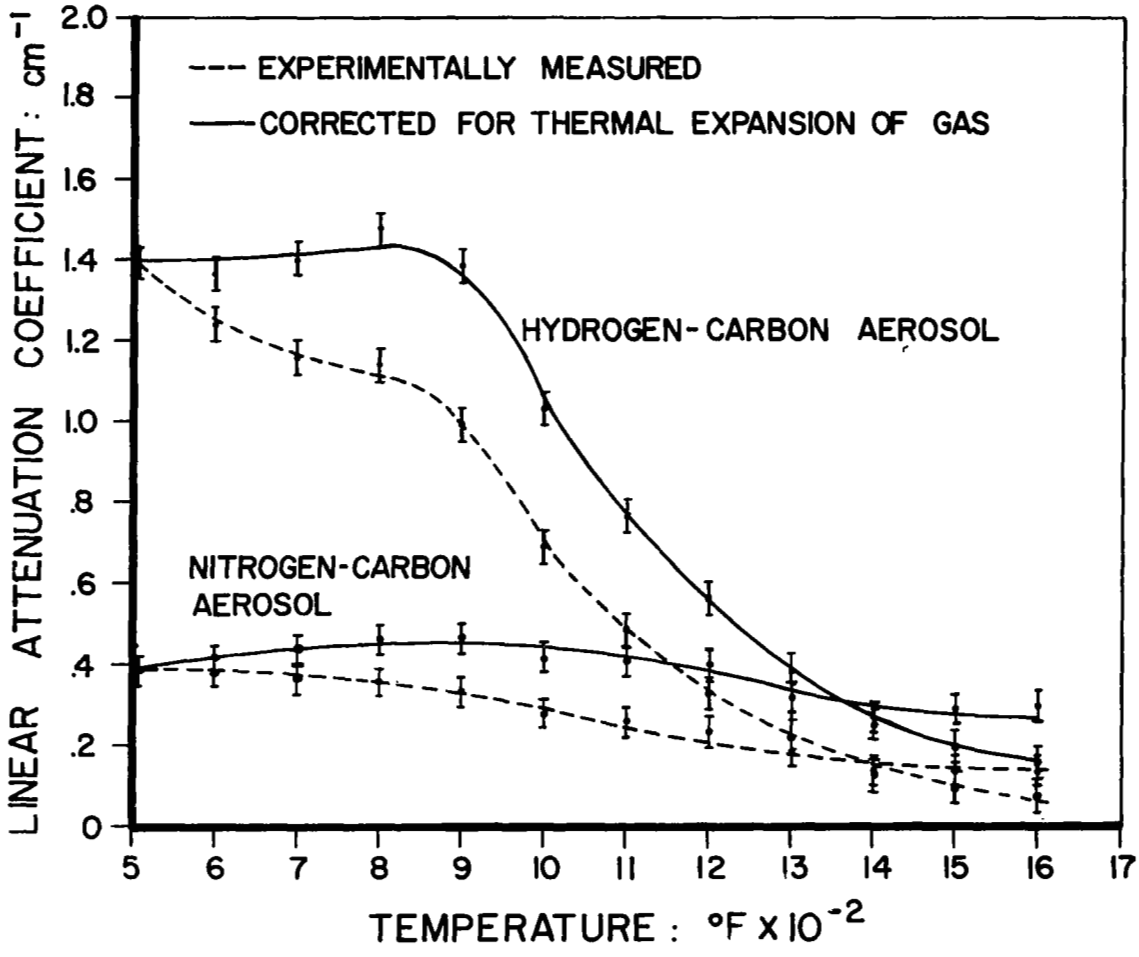

Figure 8. Linear Attenuation Coefficient of Carbon-Hydrogen and Carbon-Nitrogen Aerosols

cally at temperatures above 1000°F compared to that of a nitrogen-carbon aerosol.

Since at higher temperatures part of the carbon apparently undergoes chemical reaction, it is important to know roughly the percent of the carbon that has reacted at a given temperature. This is done by simultaneously sampling the aerosol before it enters the furnace and after it is heated in the furnace. From the difference in the aerosol concentration before and after heating, the percentage of carbon which has reacted is calculated. Figure 9 presents measured values of the percentage of carbon which has reacted as a function of temperature. It is seen that some carbon has reacted even at relatively low temperatures near 1000°F.

In order to confirm that chemical reactions between carbon and hydrogen had taken place in the carbon-hydrogen aerosol heated in the furnace, an effort was made to detect methane in the effluent. A sample of hydrogen heated with carbon particles was passed through a water-cooled sampling tube. After the mixture cooled, the carbon particles were separated both by an electrostatic precipitator and a fiberglass filter before the hydrogen was collected in the sampling tube. The sampling system was evacuated initially to remove traces of water and other gases. The collected sample was analyzed with a mass spectrograph. Peaks were observed at various atomic numbers for the constituents present in the sample. A distinct methyl group was detected at atomic numbers of 15 and 16 thereby confirming the chemical reaction between hydrogen and submicron-sized carbon particles. Precautions were taken to insure that there was no methane contamination of the hydrogen, seed material, experimental apparatus, or mass spectrograph.

The extinction parameter of tungsten particles was measured for 0.04 micron and 0.2 micron diameter particles dispersed in hydrogen. The extinction parameter of 0.20 and 0.04 micron tungsten particles is presented as a function of radiation wavelength in Figure 10 at a temperature of 80°F. The extinction parameter for spherical tungsten particles of diameters of 0.02, 0.1, and 0.2 micron was calculated using the Mie theory and is also presented in Figure 10. The electron micrographs in Appendix B indicate that the tungsten particles are highly irregular in shape and are a mixture of different sizes.

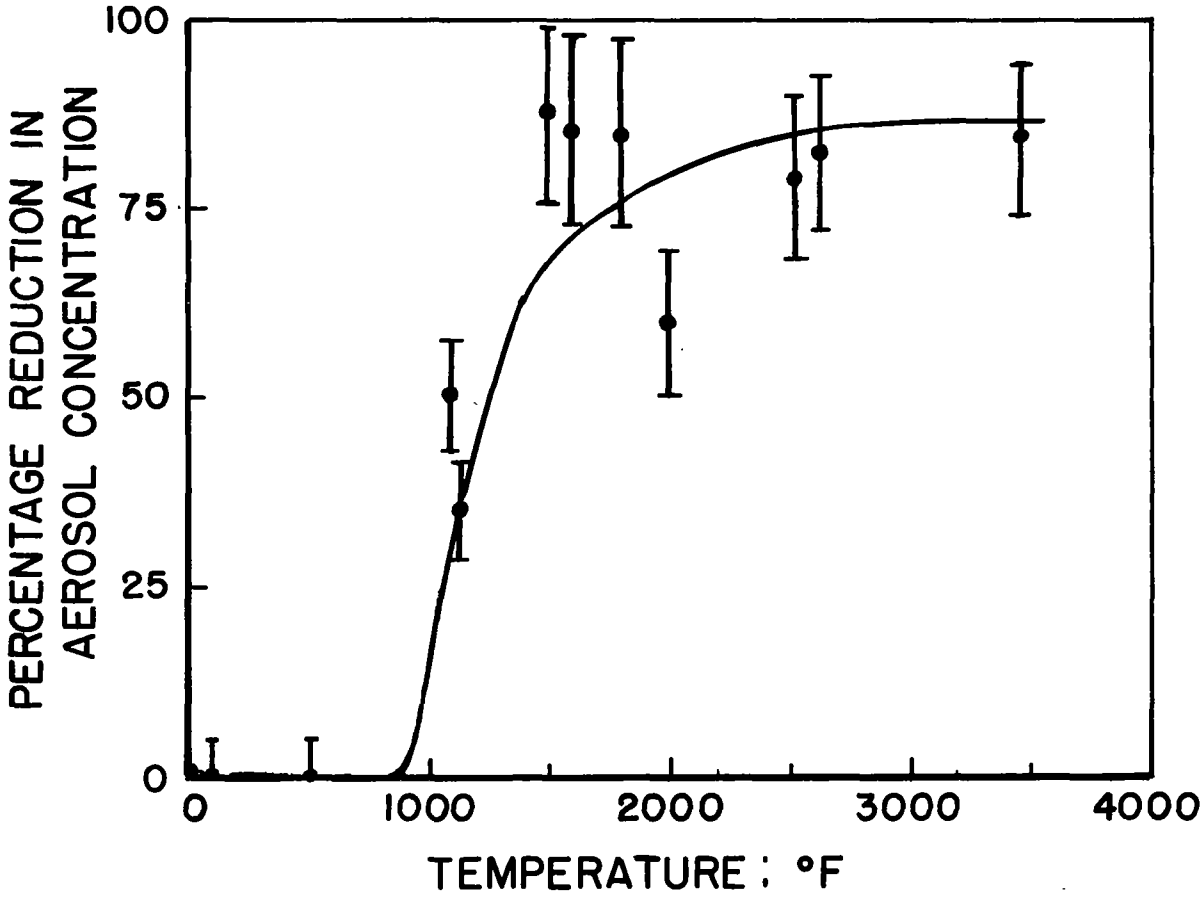

Figure 9. Percentage Reduction in Aerosol Concentration

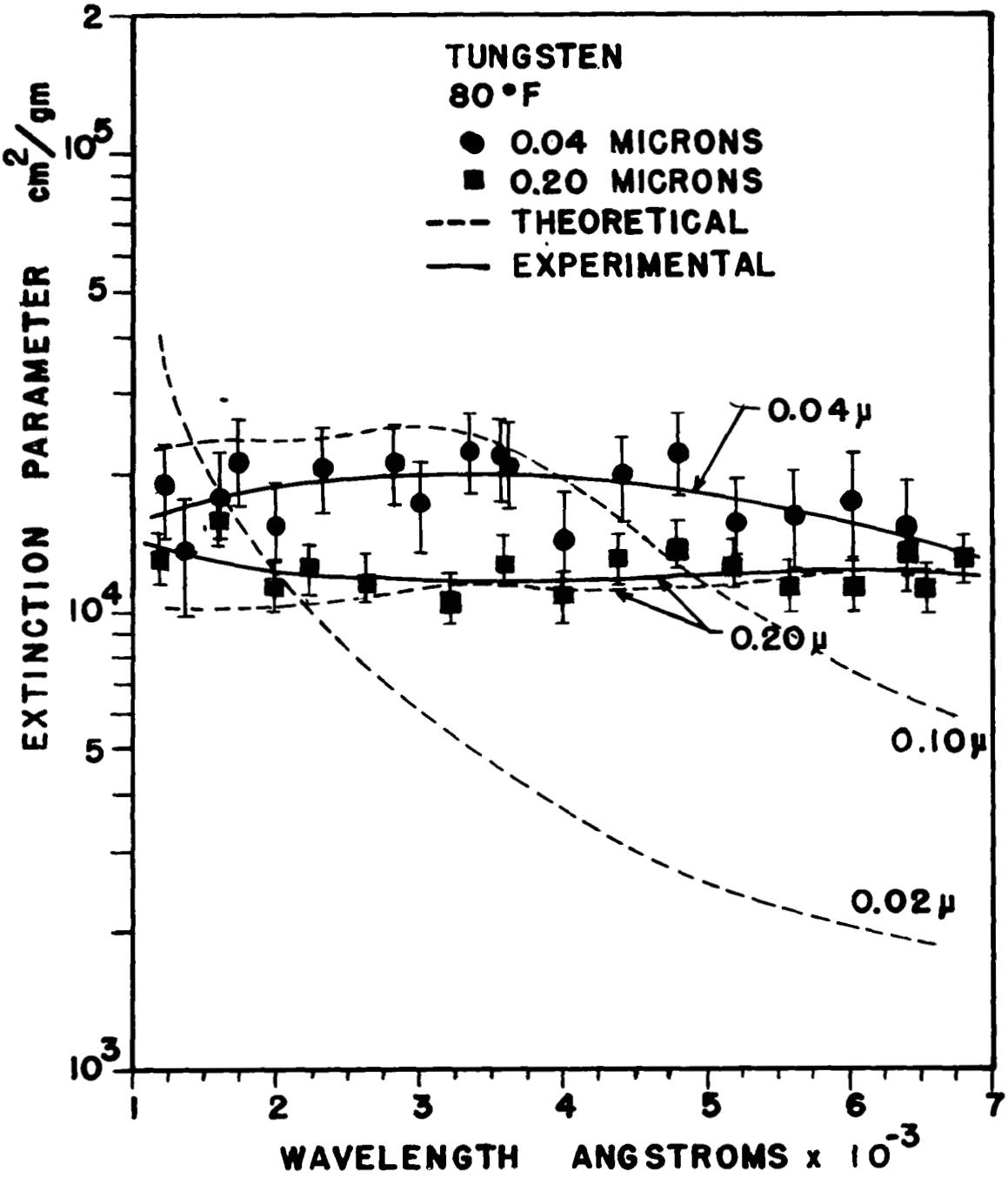

Figure 10. Comparison of the Theoretical Extinction Parameter of Tungsten Particles with Experimental Values.

As in the case of carbon, the extinction parameter of tungsten was found to be essentially independent of wavelength over the range of wavelengths and temperatures investigated. The extinction parameter of tungsten is about 20,000 cm^2/gm compared to carbon which has a value of about 50,000 cm^2/gm. In Figure 11, the extinction parameter of tungsten of 0.04 micron diameter is presented as a function of radiation wavelength at temperatures of from 80°F to 3000°F. The theoretical extinction parameter is also plotted. It has been found that tungsten particles of 0.2 micron have a lower extinction parameter compared to 0.04 micron particles.

Mie theory calculations indicate that silicon particles have a higher extinction parameter than carbon or tungsten for radii below 0.1 micron. The extinction parameter of submicron-sized silicon particles in hydrogen was measured at room temperature and the results are presented in Figure 12. The extinction parameters for spherical silicon particles of diameters of 0.1 and 0.2 micron were calculated using the Mie theory and are also presented in Figure 12 over a limited wavelength range. As in the case of tungsten, silicon particles are strong scatterers so the extinction parameter is larger than the absorption parameter[20]. Also, the electron micrographs indicate that the particles are nonspherical and are of various sizes. The submicron-sized silicon particles investigated have an extinction parameter of about 65,000 cm^2/gm which is independent of wavelength over the wavelength range investigated.

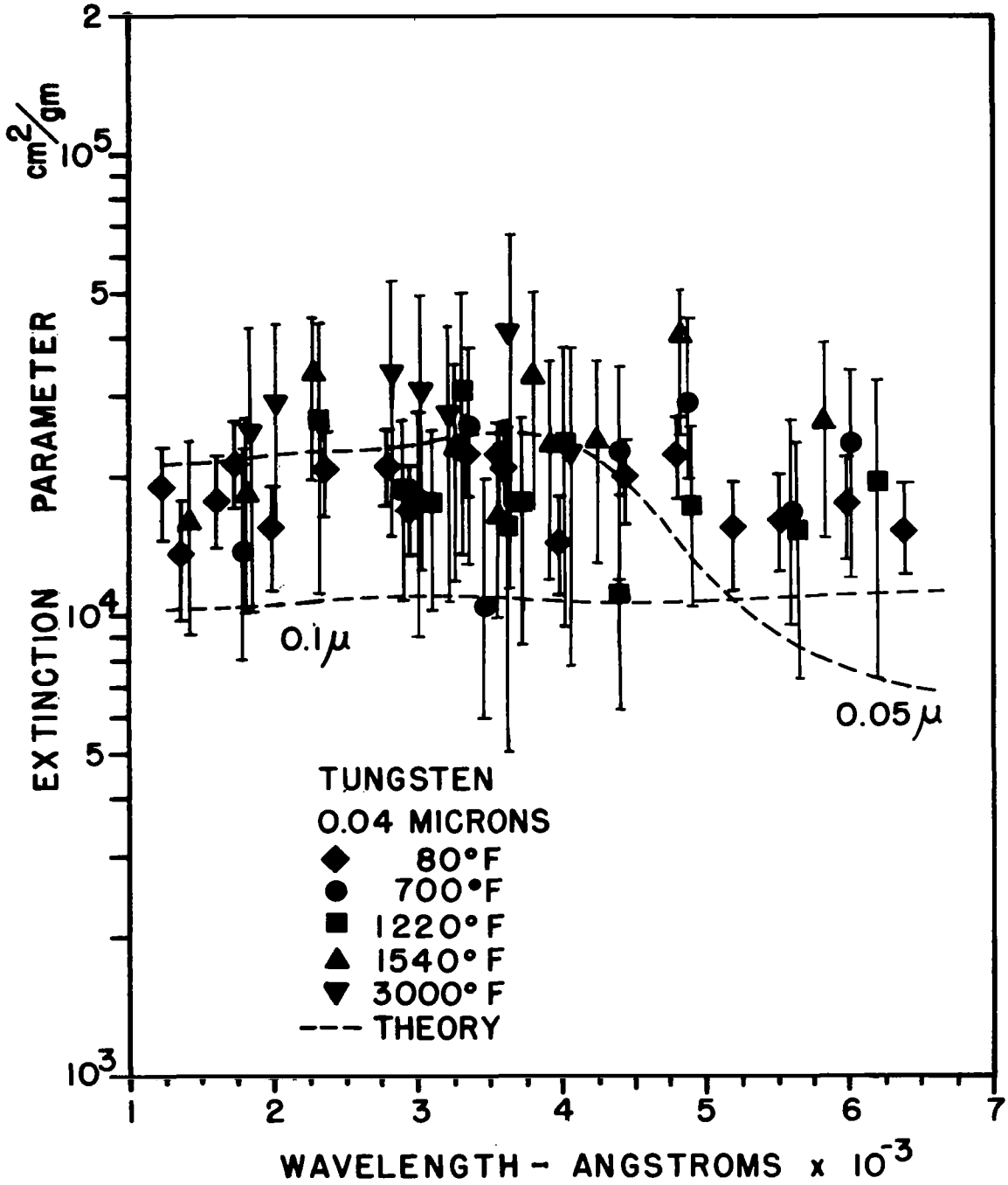

Figure 11. Comparison of the Theoretical Extinction (Absorption + Scattering) Parameter of Tungsten Particles with Experimental Values

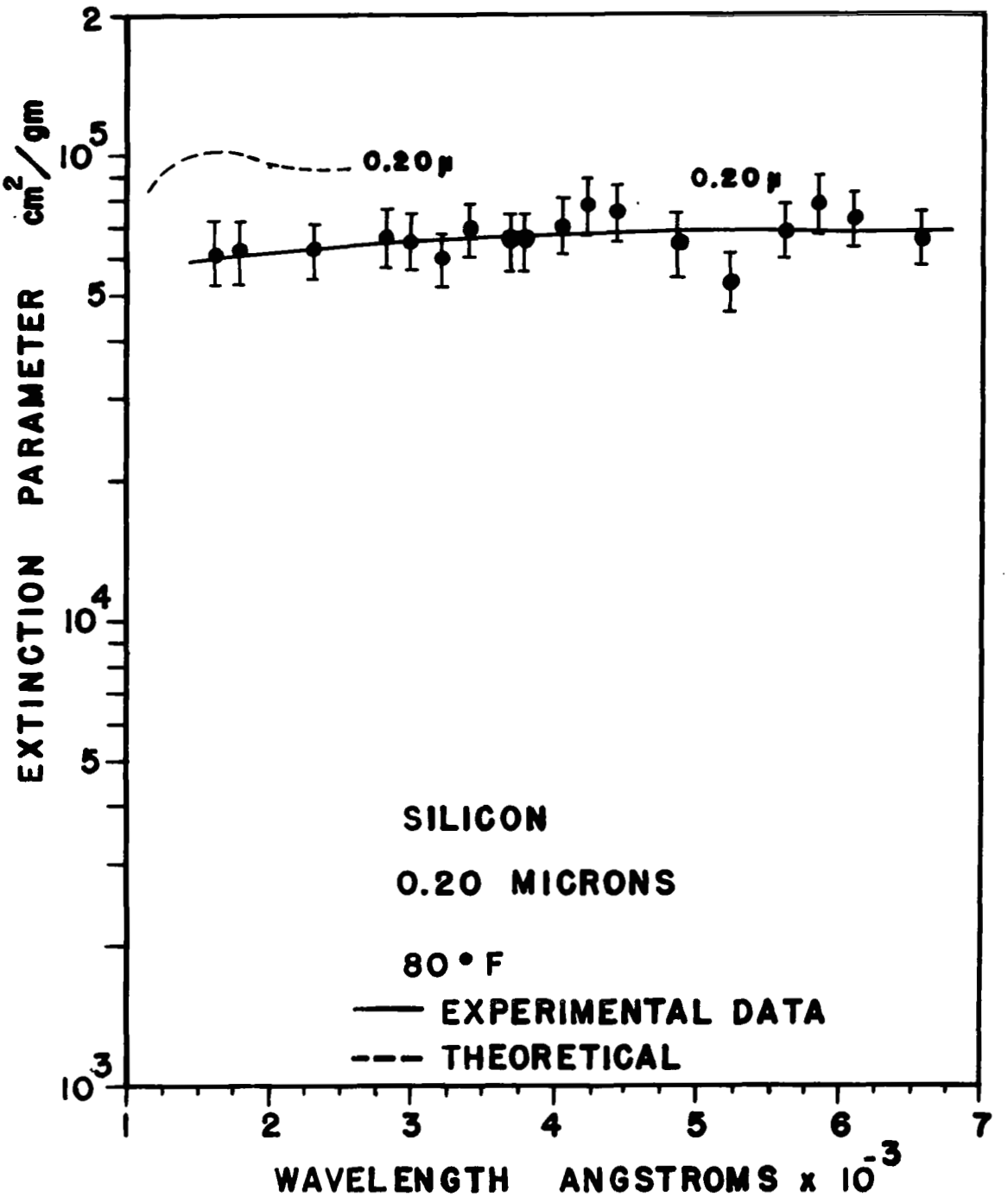

Figure 12. Extinction Parameter of Silicon Particles at 80°F

CONCLUSIONS

The purpose of this research was to measure the extinction parameter of hydrogen seeded with submicron-sized particles of various seed materials at elevated temperatures. The measured values have been compared with values calculated using Mie's theory.

Submicron-sized carbon particles with diameters of 25 millimicrons and less have a high extinction parameter of the order of 50,000 cm^2/gm which is relatively independent of wavelength and temperature over the wavelength range from 1200 Å to 6000 A and temperatures up to 3500°F. The extinction parameters calculated using the Mie theory indicate that there is a wavelength dependence for particles of a single size. However, the extinction parameter of a real cloud of particles may correspond to particles of many different sizes such that the sum is essentially wavelength independent. Also, one must remember that in the real case the particles generally are not spheres but are irregularly shaped.

At higher temperatures, a large fraction of the carbon disappears due to chemical reactions between hydrogen and carbon. This is undesirable if carbon is to be used as a seeding material in the gaseous core nuclear rocket engine because as the carbon disappears the aerosol becomes more and more transparent, thereby defeating the purpose of seeding the propellant. One method of overcoming this difficulty may be by using carbon particles of larger diameters which will react with hydrogen more slowly. The larger particles would have a smaller extinction parameter.

Other seed materials that have been investigated are submicron-sized tungsten and silicon powders. In the case of tungsten particles, the extinction parameter varies from 10,000 cm^2/gm to 20,000 cm^2/gm depending upon the average size of the particles. Unlike carbon, tungsten particles do not disappear at high temperatures. The experimental values of the extinction parameter are independent of wavelength and temperature over the range of wavelengths and temperatures investigated. The absorption and extinction parameters of tungsten particles calculated using the Mie theory indicate that they are independent of temperature up to 2420°F.

The submicron-sized silicon particles at room temperature have a higher extinction parameter than carbon and tungsten. The Mie theory indicates that

this is only true when the particle radii are below 0.1 micron. As the particle size increases, the extinction parameter drops more rapidly than for carbon, so for particle sizes above 0.1 micron, carbon has a higher extinction parameter than silicon. The experimentally measured extinction parameter is about 65,000 cm^2/gm.

The measured values of the extinction parameters are not in direct agreement with theoretically calculated values for spherical particles of a single size. This is because, as the electron micrographs illustrate, the particles are generally highly irregular in shape and are of various sizes.

APPENDIX A

PROPERTIES OF SEED MATERIALS

Carbon

Source: Cabot Corporation

	Spheron 6	Carbolac 2	Sterling MT
Smallest particle diameter	0.025 μ	0.012 μ	0.250 μ
Surface area	110 sq meters per gram	850 sq meters per gram	7 sq meters per gram
Fixed carbon	95%	87%	99.5%
Volatile content	5%	13%	0.5%
Bulk density	22lb/cft	6 lb/cft	33 lb/cft

Tungsten

Source: Vitro Laboratories	
Color : Black to gray	
Smallest particle diameter	0.04 to 0.2 micron
Bulk density	from 1 to 3 gm/cc
Surface area	4 to 6 sq meters/gm
Stability	finer sizes pyrophoric in air
Particle shape	irregular

Silicon

Source: Consolidated Astronautics

Purity: 98%

Mesh size: -200

APPENDIX B

ELECTRON MICROGRAPHS OF AEROSOL PARTICLES

Electron micrographs of various seed materials taken under various operating conditions are shown in Figures 13 through 15. An aerosol of submicron-sized particles can be produced by a number of different methods. Particles can be collected on a microscope grid from an aerosol in a number of ways. The electrostatic precipitation method gives a quite representative sample of particles. The samples shown in Figures 13-15 were obtained by the electrostatic method. The aerosols in Figures 13 and 14 were produced by passing nitrogen through a test tube containing the seed material.

Figure 13 shows the electron micrographs of carbon particles of four different varieties taken under the same magnification. In Figure 14, electron micrographs of tungsten, tungsten carbide, silicon, and silicon carbide are shown under the same magnification. Figure 15 illustrates the difference between tungsten particles produced with and without the nozzle

Carbolac 2: 0.012 Micron.

Black Pearls: 0.025 Micron.

Spheron 6: 0.025 Micron.

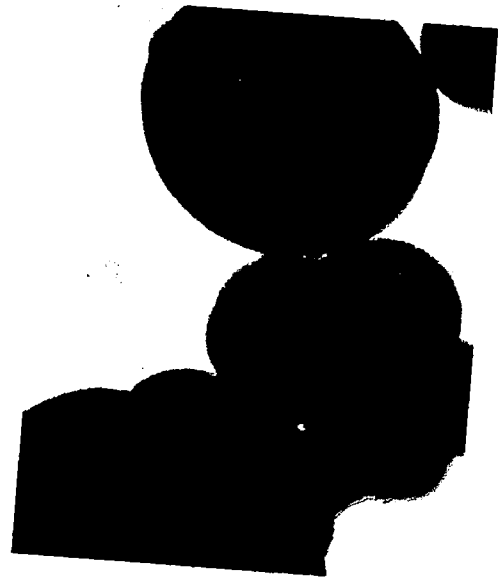

Sterling M.T.: 0.250 Micron.

0.1 Micron.

Figure 13. Electron Micrographs of Various Types of Carbon Particles

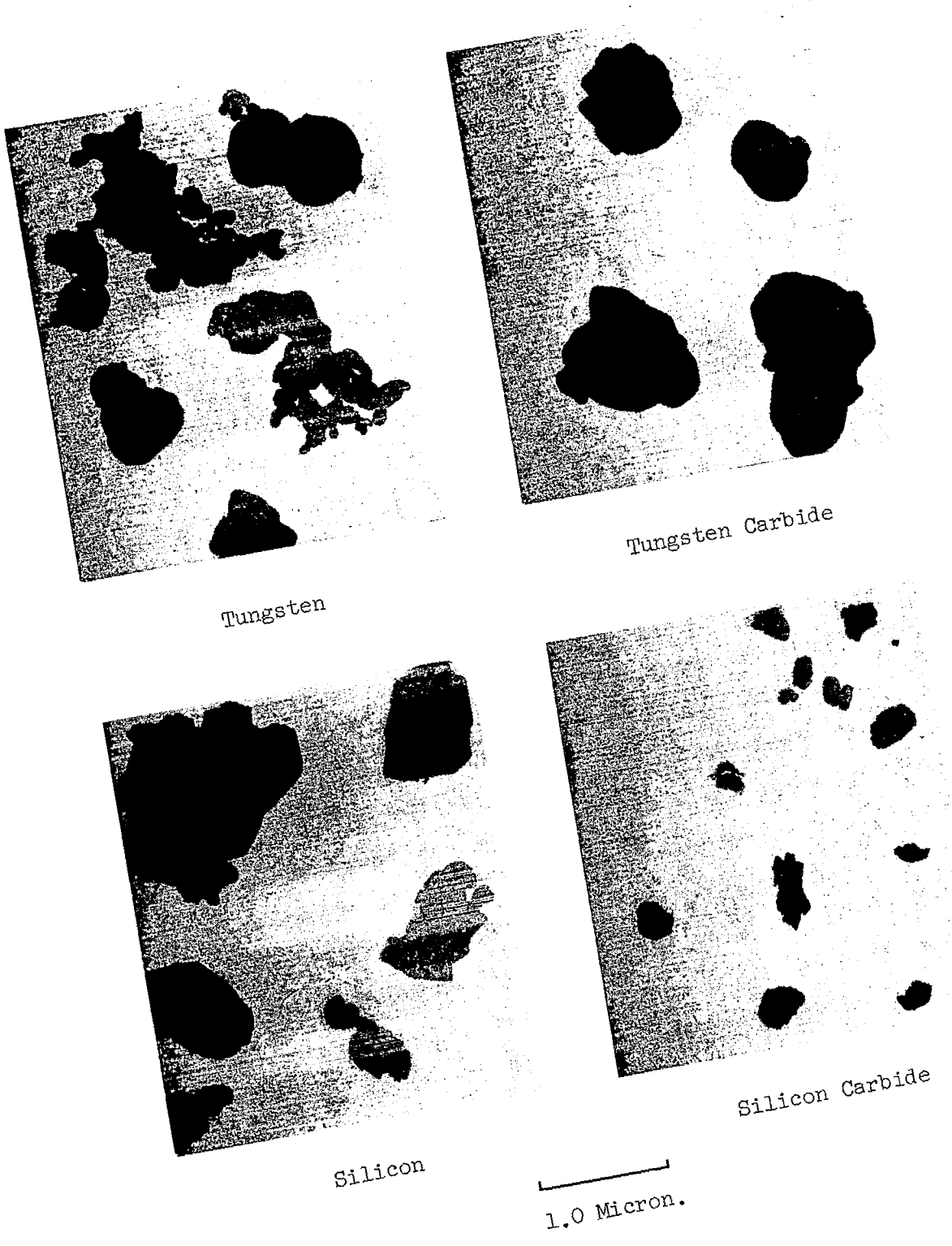

Electron Micrographs of Various Seed Materials

Without Deagglomeration.

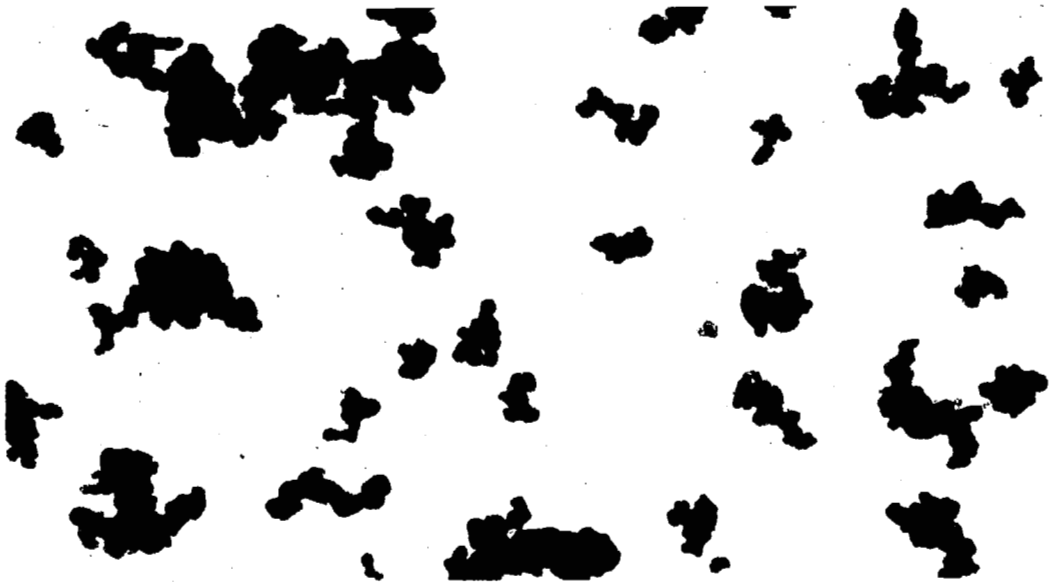

With Deagglomeration.

0.1 Micron.

Figure 15. Electron Micrographs of Tungsten Particles With and Without Deagglomeration

REFERENCES

1. Masser, C.C., "Radiant Heating of a Seeded Gas in a Coaxial Flow Gaseous Reactor," NASA TN-D-3197, January 1966.

2. Knapp, D.E., Burkig, V.C., and Cory, J.S., "Flash Heating of Seeded Gases," AIAA 3rd Propulsion Joint Specialist Conference, AIAA Paper No. 67-501, July 1967.

3. Moeckel, W.E., "Propulsion Systems for Manned Exploration of the Solar System," Astronautics and Aeronautics, 7, No. 8, August 1969.

4. Lanzo, C.D., "A Flow Experiment on a Curved-Porous Wall Gas-Core Reactor Geometry," NASA TM-X-1852, August 1969.

5. Ragsdale, R.G. and Rom, F.E., "Gas Core Reactor Work at NASA/Lewis," AIAA Paper No. 67-499, June 1967.

6. Ragsdale, R.G. and Lanzo, C.D., "Some Recent Gaseous Reactor Fluid Mechanics Experiments," AIAA Paper No. 69-477, June 1969.

7. McLafferty, G.H. and Bauer, H.E., "Studies of Specific Nuclear Light Bulb and Open Cycle Vortex-Stabilized Gaseous Nuclear Rocket Engines," UACRL Report No. F-910093-37, September 1967.

8. Lathan, T.S., "Nuclear Studies of the Nuclear Light Bulb Rocket Engine," United Aircraft Corporation Research Laboratories Report No. G-910375-3, September 1968.

9. Williams, J.R., Shenoy, A.S., and Clement, J.D., "Radiant Propellant Heating in the Gaseous Core Nuclear Rocket," AIAA 4th Propulsion Joint Specialist Conference, AIAA Paper No. 68-572, June 1968.

10. Hunter, M.W., Jr., "Single Stage Spaceships Should Be Our Goal," Nucleonics Handbook of Nuclear Research and Technology, McGraw-Hill, N.Y., 1966.

11. Cooper, R.S., "Nuclear Propulsion for Space Vehicles," Annual Review of Nuclear Science 18, 203-28, 1968.

12. Van de Hulst, H.C., Light Scattering by Small Particles, John Wiley & Sons, New York, 1957.

13. Born, M. and Wolf, E., Principles of Optics, Third Edition (revised), Pergamon Press, 1965.

14. Krascella, N.L., "Theoretical Investigations of the Absorption and Scattering Characteristics of Small Particles," United Aircraft Research Laboratories Report C-910092-1, September 1964.

15. Lanzo, C. D. and Ragsdale, R. G., "Experimental Determination of Spectral and Total Transmissivities of Clouds of Small Particles," NASA TN-D-1405, September 1962.

16. Williams, J. R., Clement, J. D., Shenoy, A. S., Partain, W. L. and Jacobs, W. R., "The Attenuation of Radiant Energy in Hot Seeded Hydrogen," Georgia Institute of Technology, Project A-1045, Status Report No. 3, May 1969.

17. Mie, G. A. F. W. L., "Beitrage zur Optik truber Medien, Speziell Kolloidaler Metallosungen," Annal d. Physik, 25, 377, 1908.

18. Davies, C. N., "Survey of Scattering and Absorption of Light by Particles," British Journal of Applied Physics, Supplement No. 3, 64-65, 1954.

19. Aden, A. L., "Electromagnetic Scattering from Spheres with Sizes Comparable to the Wavelength," Journal of Applied Physics, 22, No. 5, 601-5, 1951.

20. Williams, J. R., Shenoy, A. S., Clement, J. D., "Theoretical Calculation of Radiant Heat Transfer Properties of Particle-Seeded Gases," NASA CR-1505, 1970.

21. Svatos, J., "Light Scattering by Flattened Ellipsoids," Astronomical Institute of Czechoslavakia Bulletin, 18, No. 2, 114-19, 1967.

NASA-Langley, 1970 —— 33 **E-5405**